ELSEVIER

PII S0360-3016(00)01494-2

HYPOXIA IN HUMAN INTRAPERITONEAL AND EXTREMITY SARCOMAS

Sydney M. Evans, V.M.D.,* Stephen M. Hahn, M.D.,[†] Deirdre P. Magarelli, B.S.,*
Paul J. Zhang, M.D.,[†] W. Timothy Jenkins, M.S.,[†] Douglas L. Fraker, M.D.,[†]
R. Alex Hsi, M.D.,[‡] W. Gillies McKenna, M.D., Ph.D.,[†] and Cameron J. Koch, Ph.D.[†]

From the Schools of *Veterinary Medicine and [†]Medicine, University of Pennsylvania, Philadelphia, PA; [‡]Virginia Mason Medical
Center, Seattle, WA

Purpose: The presence of hypoxia, measured by needle electrodes, has been shown to be associated with poor patient outcome in several human tumor types, including soft tissue sarcomas. The present report emphasizes the evaluation of hypoxia in soft tissue sarcomas based upon the binding of the 2-nitroimidazole drug EF5 (2-{2-nitro-1H-imidazol-1-yl}-N-(2,2,3,3,3-pentafluoropropyl) acetamide). EF5 has previously been shown to be predictive of radiation response in animal tumors and in *in vitro* studies. We have also previously reported studies of EF5 binding in human squamous cell tumors. Using fluorescent immunohistochemical techniques, we provide data on the presence and distribution of EF5 binding, as a surrogate for hypoxia, in human spindle cell tumors.
Methods and Materials: Patients with spindle cell tumors who were scheduled for tumor surgery were asked to participate in the Phase I trial of EF5. Approximately 48 h preoperatively, EF5 was administered i.v. at doses between 9 and 21 mg/kg. Binding in frozen sections of biopsied tissues was determined using monoclonal antibodies labeled with the green-excited, orange-emitting fluorescent dye, Cy3. Calibration studies were performed *in vitro* by incubating fresh tumor tissue cubes obtained from each patient with EF3 (an analog of EF5) under hypoxic conditions ("reference binding"). The goal of these calibration studies was to quantify the maximal binding levels possible in individual patient's tissues. The relationship between binding (*in situ* based on EF5 binding) and reference binding (*in vitro* based on EF3 binding) was determined.
Results: Eight patients were studied; 3 of these patients had gastrointestinal stromal tumors (GIST). The incubation of tumor tissue cubes in EF3 under hypoxic conditions demonstrated that all tumors bound drug to a similar extent. Reference binding showed a 3.2-fold variation in median fluorescence (113–356) on an absolute fluorescence scale, calibrated by a Cy3 dye standard. *In situ* binding in the brightest tumor section varied by a factor of 25.4 between the lowest and highest binding tumor (7.5–190.2). Heterogeneity of highest binding was greater between tumors than within individual tumors. A correspondence between EF5 binding and Eppendorf needle electrode studies was seen in the 5 patients with non-GISTs.
Conclusion: Inter- and intratumoral heterogeneity of EF5 binding in spindle cell tumors has been documented. Patterns of binding consistent with diffusion limited hypoxia are present in human spindle cell neoplasms. © 2001 Elsevier Science Inc.

EF5, Hypoxia, Sarcoma, Human, Nitroimidazole, Immunohistochemistry.

INTRODUCTION

The assessment of hypoxia in human tumors has been a subject of intense interest in recent years. The ability to diagnose hypoxia (1) was considered important in radiation therapy because this could help direct dose prescription, the use of hypoxic cell modifiers (for example, see Refs. 2 and 3), or blood flow/oxygen-modifying therapies (for example, see Ref. 4). Recently, the paradigm that hypoxia was important because it limited radiation response was expanded when it was observed that patients treated with *surgery alone* for uterine cervix cancers had a better prognosis for local control if their tumors were better oxygenated preop-

eratively (5). These observations led to the suggestion that hypoxic uterine cervix tumors were intrinsically more biologically aggressive than well oxygenated ones. Further support for this idea was provided by a study of high-grade extremity soft tissue sarcomas (STS), demonstrating that these cancers were more likely to metastasize if they were hypoxic at the time of initial therapy (6). Molecular studies support the association of aggressive tumor phenotypes with the presence of hypoxia (7–9).

The clinical measurements of hypoxia described above were performed using needle electrode techniques. We have previously reported the use of another clinically relevant

method for measuring tumor hypoxia *in vivo*, e.g., binding of the 2-nitroimidazole drug, EF5. We have shown this technique to be accurate in the correlation of binding with independent measurements such as radiation response (10), blood flow (11), blood pO_2 as determined by phosphorescence decay (12), therapeutic manipulations (13), tirapazamine response (14), and paired survival assays (15). In human patients, EF5 has been shown to be nontoxic (16) with up to 70% excreted unchanged in the urine (17). One advantage of this methodology is the ability to detect binding on a cell-to-cell basis, using both fluorescent immunohistochemical imaging techniques (18) and/or flow cytometric techniques (19).

Based on these considerations, we have studied the oxygen content of human spindle cell tumors in i.p., extremity, trunkal, and retroperitoneal sites. The presence and distribution of hypoxia was analyzed using immunohistochemical imaging of EF5 binding and Eppendorf needle electrode measurements. The inter-relationships between EF5 binding studies, needle electrode studies, and tumor histology are discussed herein.

METHODS AND MATERIALS

Human subjects

In February 1998, EF5 was granted IND status for use in human cancer patients by the FDA, and the Phase I protocol was approved by the University of Pennsylvania Institutional Review Board. Written informed consent was obtained from all patients entered on this study. Eligible patients were those undergoing incisional or excisional tumor biopsies for other medical or surgical indications. Patients of all ethnic and gender groups were included. Exclusion criteria emphasized a history of grade III or IV peripheral neuropathy as defined by the National Cancer Institute Division of Cancer Treatment (NCI/DCT) Common Toxicity Criteria because neurotoxicity has been reported in the studies of 2-nitroimidazole compounds used in high, multiple doses as hypoxic cell sensitizers (for example, see Ref. 20). Pregnant patients, patients less than 18 years of age, and those who were HIV positive were excluded.

Drug administration and toxicity

EF5 was supplied by the NCI/DCT in 100-mL vials. The solvent was water into 2.5% alcohol, and each milliliter contained 3 mg EF5 and 5 mg dextrose. EF5 was administered i.v. via a peripheral catheter at a rate of approximately 350 mL/h. Acute toxicity was assessed using NCI/DCT Common Toxicity Criteria. Patients were examined for signs and symptoms of toxicity at approximately 1 h, 48 h, and 28 days following drug infusion. At the time of EF5 infusion and approximately 28 days later, blood chemistries and blood counts were performed.

Tissue acquisition

Approximately 48 h (range 40–55) following drug administration, the tumor was either biopsied or resected.

When possible, preceding extensive surgical manipulation, sterile tumor tissue was obtained and placed in iced EX-CELL 610 media (JRH Biosciences, Kansas) with 15% fetal calf serum. These tissues were immediately returned to the laboratory, where they were processed to obtain cells for tissue culture and flow cytometric analysis, and tissues to determine reference EF3 binding (see below). Any extra sterile tissues were placed on moist filter paper, coated with a thin layer of Tissue Tek™ OCT compound (Sakura Finetek USA, Inc., Torrence, CA) and frozen on dry ice, as previously described (16). At the completion of surgery, the tumor specimen was taken to the department of pathology where additional tumor and, if available, normal adjacent tissues were obtained. These tissues were frozen, as above, until they were probed for EF5 binding.

Determination of tissue reference binding

The purpose of these studies was to determine the maximum binding rate of the tissue *in vitro* using EF3 and low (0.2%) oxygen concentrations. This value will be referred to as "reference binding." The rationale for use of EF3, as well as the technical aspects of determining reference binding, has been previously described (16). Briefly, tissue cubes were diced from tissue slices and placed into each of two vials. Control tissue cubes were shaken at 37°C in medium without EF3. Reference cubes were similarly incubated for 3 h with 200 μM EF3 and a gas phase containing 0.2% oxygen. After incubation, the samples were frozen on dry ice until sections could be collected and stained with ELK5-A8 antibodies.

Immunohistochemical staining and photography of tissues for EF3 and EF5 binding

Frozen tissues that were exposed to EF5 *in situ* were brought to −20°C one-half hour before sectioning. Sections were made at 10 μm, fixed, blocked and stained with ELK3-51 antibody conjugated with Cy3 dye (75 μg/mL) as previously described (21). Adjacent sections were treated without antibody ("no stain") and with 75 μg/mL antibody admixed with 0.5 mM EF5 ("competed stain") to assess endogenous tissue fluorescence and nonspecific binding of the antibody, respectively. The competed stain sections were rinsed with buffer containing 0.25 mM EF5. The technique for immunohistochemistry of EF3 adducts in tissue cube studies was identical to that for EF5, with the exception that ELK5-A8 antibody was used.

Epifluorescence measurements were made on the stained slides using a Nikon LabPhot microscope with 100-W high-pressure mercury arc lamp. Filter cubes were optimized for wavelengths of interest (Omega Optical, Vermont). A cooled (−25°C) CCD digital camera (Photometrics "Quantix," KF1400, Grade I defects) was attached to the microscope via a Diagnostic Instruments HRP060 C-mount adapter. Residual infrared light from the filter cubes was eliminated by two serial XF86 filters (Omega Optical) at the base of the C-mount. The manual stage of the microscope was replaced by a Ludl Electronic Products 99S000 auto-

matic stage with 0.1 μm step size. The camera and stage were controlled by a Macintosh 9600 Power PC computer. Software was Scanalytics "IP Laboratory," a general purpose image analysis program with modular support of the hardware components.

During photography, tissue sections were covered by a hemocytometer coverslip separated from the section by strips of mylar tape and the enclosed space filled with phosphate-buffered saline (PBS). This provides a uniform optical path and prevents tissue desiccation, which can change the apparent levels of fluorescence.

For each patient, at least two tumor regions and two levels within each region (separated by 0.5 mm) were examined for regions of *in situ* EF5 binding. The tissue cube sections were scanned for the section(s) with highest EF3 binding and these sections were imaged. The imaged regions were evaluated using a 10× microscope objective (field size set electronically at 1.05×0.7 mm^2) and, typically, nine fields were examined for each *in situ* section. It was usually possible to photograph a tissue cube section in a single field. To improve camera sensitivity while still providing multiple pixels per cell, each image field consisted of 600×400 pixels. Each of these was a 2×2 bin of the actual camera chip pixels, with 12-bit gray scale resolution.

Immunohistochemical staining for CD31/PECAM

Some tissue sections were stained first for CD31 and subsequently for EF5 to determine the spatial relationship between hypoxia and blood vessel distribution. A protocol allowing primary staining by a mouse monoclonal to human CD31 followed by labeled secondary rat anti-mouse antibody was used. The secondary antibody labeling allowed detection by peroxidase stain or fluorescence. Because subsequent staining with mouse monoclonal antibodies against EF5 adducts would disrupt the rat anti-mouse secondary labeling for CD31, a short fixation step was added (4% paraformaldehyde, 20 min at room temperature) before standard rinsing, blocking, and staining for EF5 adducts.

Quantification and analysis of EF5 binding based on immunohistochemistry

To quantitatively assess *in situ* EF5 binding, an absolute fluorescence scale was required. The fluorescence of a reference thickness of Cy3 dye was determined at the beginning and end of every imaging procedure. The dye standard consisted of Cy3 dye in PBS with 1% paraformaldehyde injected into a standard hemocytometer (thickness of the dye layer = 100 μm). The absorbency of the dye was 1.25 at 549 nm. The dye was imaged (focusing on the gridlines of the hemocytometer) and the exposure time and average pixel intensity noted. This fluorescence value was assigned a value of 1,000. Most tissues examined had maximal fluorescence less than the dye standard. The absolute fluorescence of any sectional region of interest was obtained by determining actual pixel intensity, dividing by the pixel intensity of the standard, and then multiplying by 1,000

times the ratio of exposure times for dye standard and region of interest. The final absolute fluorescence was then corrected for the area under the curve (AUC) for individual patients, based on blood samples that were taken at the completion of the EF5 infusion and at the time of surgery. This pharmacokinetic data are reported separately (17) but show that the initial blood level is proportional to injected dose and the AUC can be predicted based on initial dose and blood concentration at the time of surgery.

Multiple fields representative of the entire section were imaged as described above. In this assessment of tissue binding, we have considered the average pixel intensity in the region of brightest binding as a representation of the most hypoxic cells. Individual bright cells in the center of necrotic regions were excluded because they were considered to be nonclonogenic and would therefore not impact upon treatment response.

Light microscopic evaluations

Slides stained for EF5 binding were counterstained with hematoxylin and eosin and evaluated by a pathologist (PZ) to assess the presence of tumor and/or normal tissue. Detailed evaluation of paraffin embedded tumor specimens (from the primary resection specimen) were performed and the following characteristics were evaluated: mitosis (number per 10 high-power fields), percentage necrosis, and grade. Overall tumor size was also noted.

Eppendorf measurements

Tumor oxygenation was measured in anesthetized patients using a polarographic needle electrode (pO$_2$ Histograph; Eppendorf-Netherler-Hinz, GmbH, Hamburg, Germany). Inhaled oxygen content was between 21% and 30% at the time of pO$_2$ probe placement. All measurements were performed under direct tumor visualization and 2–4 separate locations were sampled. Track length was adjusted to the tumor size; step size was 0.4 mm.

RESULTS

Patients, drug administration, and toxicity

Between March 1, 1998 and July 31, 1999, 20 patients signed informed consent documents and participated in a Phase I trial of EF5. Eight patients had a preoperative histopathologic diagnosis of spindle cell neoplasm compatible with sarcoma. Two tumors arose in the extremity, 2 were trunkal, 1 was retroperitoneal, and 3 were gastrointestinal stromal tumors (GIST, Table 1). Patient no. 10 had an extremity sarcoma that was metastatic to the lungs at the time of surgery. Patient no. 8 had a trunkal malignant fibrous histiocytoma (MFH) that occurred in a previously irradiated mantle field for lymphoma. Four of the 5 non-GIST sarcomas were first occurrences, whereas one non-GIST and 3 GIST tumors were recurrent at the time of the EF5 study. Two of the patients with GIST were undergoing a laparoscopic procedure for restaging of their disease, hence tissue sampling was very limited. Patient no. 12 (the

Table 1. Patient information

Patient no.	Age/Sex/Race	EF5 mg/kg	Site/Histology	Stage/Grade	Other	Clinical status	Absolute binding	Cube (reference) binding	Relative binding %
2	40/F/C	9	STS—E	Low	first occurrence	LRR	19.9	142.2	14.0
8	63/M/C	12	STS—T	High	in previously irradiated site	DM	112.0	112.8	99.3
9	52/M/C	12	GIST	Low	Recurrent	PD, DOD	12.5	153.0	8.2
10	53/F/AA	12	STS—E	High	first occurrence, Metastatic to lung	DM, DOD	190.2	208.3	91.3
11	34/M/C	12	STS—T	High	first occurrence	NED	87.2	312.1	28.0
12	70/M/C	12	GIST; multiple nodules sampled	High	Recurrent	DOC	12.5–36.5	243.2	5.1–15.0
16	48/M/C	16	STS—RP	High	first occurrence	LRR	132.6	534.1	24.8
20	36/F/C	21	GIST	High	Recurrent	PD	7.5	355.5	2.1

Relative binding refers to percent of cube (reference) binding, corrected for AUC. In the patient where cube values were not available, an average EF5 value of appropriate other cubes was used. Absoute binding is on a scale of 0–1000.

Abbreviations: C = Caucasian; AA = African American; GIST = GI stromal tumor; NED = no evidence of disease; LRR = locoregional recurrence; DM = distant metastasis; PD = progressive disease; DOD = dead of disease; DOC = dead of other causes; RP = retroperitoneal; T = trunkal; E = extremity.

third patient with GIST) was undergoing a debulking procedure to remove an obstructing mass at the porta hepatica. Several nodules attached to the small intestines were also removed at the time of surgery.

All patients received EF5 over 1–2 h through an indwelling i.v. catheter. Five patients received 12 mg/kg and one patient each received 9, 16, and 21 mg/kg (Table 1). There were no clinical or biochemical, acute, or late (28 day) EF5-related toxicities reported. Patient no. 12 died 9 days postoperatively from treatment-related complications. EF5 was not implicated in the cause of death. Studies in patients with squamous cell tumors showed similar lack of toxicity (16). The dose 21 mg/kg EF5 has been approved by the NCI for studies; these data have been presented at the Spring 2000 Cancer Therapeutic Evaluation Program (CTEP) Phase I meeting. Plasma half-life of EF5 was 11.7 ± 2.6 (SD) h, irrespective of the dose of drug given (17).

Reference EF3 binding

The brightest binding cells within the cubes were identified by examining multiple sections cut consecutively from the surface of the cube. The section which contained the brightest binding were usually within 3–10 cell layers from the surface, as a result of metabolism-induced depletion of oxygen at this tissue depth (Fig. 1). The average absolute fluorescence of the brightest cube sections was determined and found to vary by a factor of 3.2, with a range of 113–356.

In situ *binding*

Multiple areas of bright binding were seen in tissue sections from four non-GIST sarcomas (patient nos. 8, 10, 11, 16; Fig. 2). Binding occurred predominantly in highly cellular areas, adjacent to regions of necrosis (patient nos.

11 and 16; Fig. 2) and occasionally in hyalinized regions (patient no. 8). Minimal binding was seen in the extremity desmoid (patient no. 2), which was highly cellular, but low grade. Intertumoral variation of the fraction of reference binding, corrected for dose of drug administered, ranged from 14.0% to 99.3% (Table 2).

GIST nodules which were less than 1-cm diameter were removed under laparoscopic guidance from patient nos. 9 and 20 contained low EF5 binding (Table 1). In patient no. 12, biopsies were taken from the large porta hepatis mass (6-cm diameter) and small bowel masses measuring 1.65 cm and 0.5 cm were excised. Binding (15% of reference) was identified in the bowel mass that was 1.65 cm, whereas less binding (5.1% of reference binding) was seen in the smaller nodule. In the central region of the porta hepatis mass, EF5 binding was 10.7% of reference binding. Multiple sections of the porta hepatis mass were examined for EF5 binding; intratumoral heterogeneity in the levels of binding were seen with regions of severe and intermediate binding present in different sections. PECAM binding was assessed in a region of intermediate hypoxia in the porta hepatis mass and compared to a region of severe hypoxia in the 1.65-cm bowel mass (Fig. 3). The patterns and distribution of hypoxia and blood vessels were quite different in these two sections. In the 1.65-cm nodule, small regions of high binding were present adjacent to regions of necrosis; patterns of diffusion limited hypoxia dominated (Fig. 3a). In contrast, in the porta hepatis mass, larger regions of moderate EF5 binding were seen and necrosis was rare. In this section, PECAM-stained vessels overlapped regions of moderate to low EF5 binding, suggesting the presence of perfusion limited hypoxia or plasma flow without red blood cells (22) (Fig. 3b).

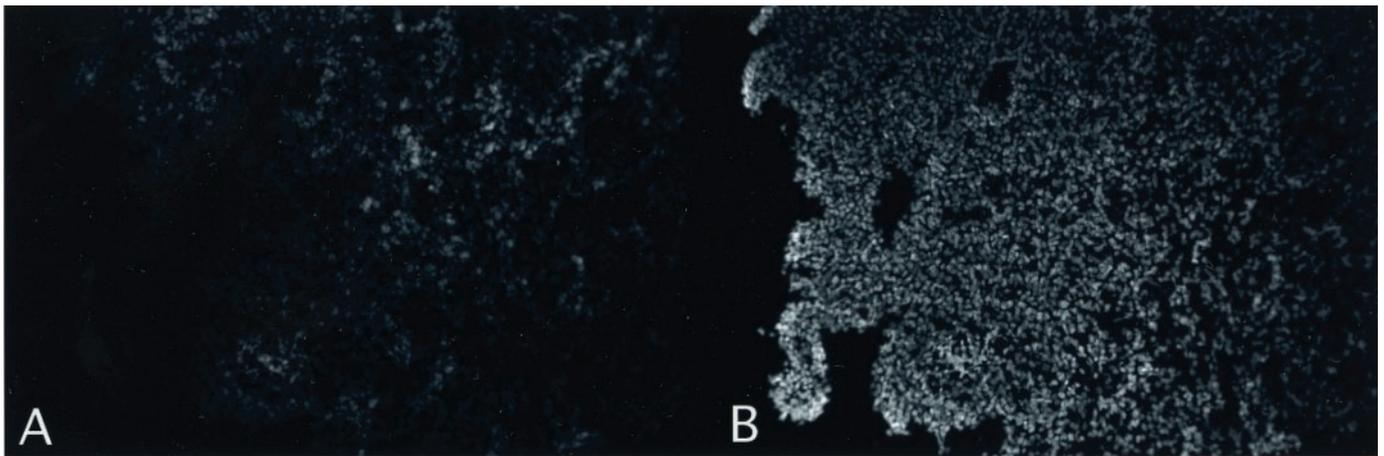We assessed the variability of the *brightest* binding be-

Fig. 1. (A) 1.0 × 0.7 mm. Photomicrographs of the brightest section from the tumor tissue cube (patient no. 16), incubated *in vitro* in 0.2% oxygen and 600 μM h EF3, for determination of reference binding. Frozen sections were stained with ELK5-A8 and the tissue section containing maximal binding was imaged. (B) The same section counterstained with Hoescht 33342 to label DNA-containing nuclei in the tissue section. The nonzero oxygen concentration in the suspension allows nonmaximal EF3 binding at the surface of the cube, to a depth of approximately 200 μm from the surface. As a result of respiration-induced severe hypoxia, maximal EF3 binding is seen at depths into the cube greater than approximately 200 μm. Thus, regions of maximal binding can be analyzed several cell layers from the cube surface, where there is less chance of tissue sectioning artifacts.

tween tissue sections (Fig. 4). At least four sections from each patient were evaluated. The variations in maximal binding within each tumor (intratumoral) were much less than the approximately 100-fold variation of intertumoral levels of binding. The intratumoral variability of *all* binding within the sections varied over a large range because all sections contained regions of very low or no binding.

Histopathologic assessments (Table 2)

Histopathologic assessments were performed on formalin-fixed tissues as well as the individual frozen sections counterstained for H&E after assessment of EF5 binding. For the latter specimens, emphasis was placed on confirming that the regions being evaluated for EF5 and EF3 binding contained predominantly tumor cells. Detailed assessment of the histologic type, tumor grade, presence and amount of necrosis, and number of mitoses per 10 high-power fields were performed on paraffin-embedded sections. Three GIST tumors, two leiomyosarcomas, and one each synovial cell sarcoma, MFH and a desmoid were identified (Table 2). Two tumors were low grade and the remaining tumors were considered high grade. There was substantial intertumoral variability in the presence of necrosis and number of mitoses (Table 2).

Eppendorf measurements (Table 3)

Eppendorf measurements were performed on five of the eight patients (Table 3). Eppendorf electrode studies were not performed in two patients with GISTs because appropriate access for the needle could not be obtained during the laparoscopic studies. In the third patient with a GIST, the tumor was adjacent to the porta hepatis and Eppendorf needle electrode studies were not performed for logistical as

well as safety reasons. All other patients studied had three or four tracks recorded. A trend between high EF5 binding and low pO$_2$ values determined by Eppendorf needle electrodes was found ($r = 0.668$; Fig. 5).

DISCUSSION

STS are relatively uncommon tumors, accounting for 7,800 new cancer cases in the United States in 1999 (23). They can occur in many sites; 50–60% of primary STS are located in the extremities, 25% in retroperitoneal and visceral primary sites, 15% in trunkal and thoracic areas, and 5% in the head and neck regions (24). Although local recurrence is more problematic in sarcomas of the torso and head/neck than in the extremities, distant failure is the most common cause of treatment failure and mortality in this patient group (25). Many clinicopathologic prognostic factors have been studied to determine which patients are at highest risk of failure. In most series, tumor size, grade (26), deep location, and positive resection margins predict local recurrence rate (24). In a series of 1,041 adult patients with extremity STS, clinicopathologic prognostic factors for early metastasis were large tumors, high-grade tumors, deep tumors, and locally recurrent disease (27). In recent years, emphasis has been placed on biologic parameters that may affect prognosis and outcome. Studies on STS have supported the prognostic importance of a number of biologic factors including proliferation indices (28), oncogene expression (28) and the presence of matrix-degrading enzymes (24). These physiologic processes, and others such as angiogenesis (29–31), metallothionein expression (32, 33), proliferation (34, 35), and necrosis (30) have been associated individually with the presence of hypoxia and outcome, but
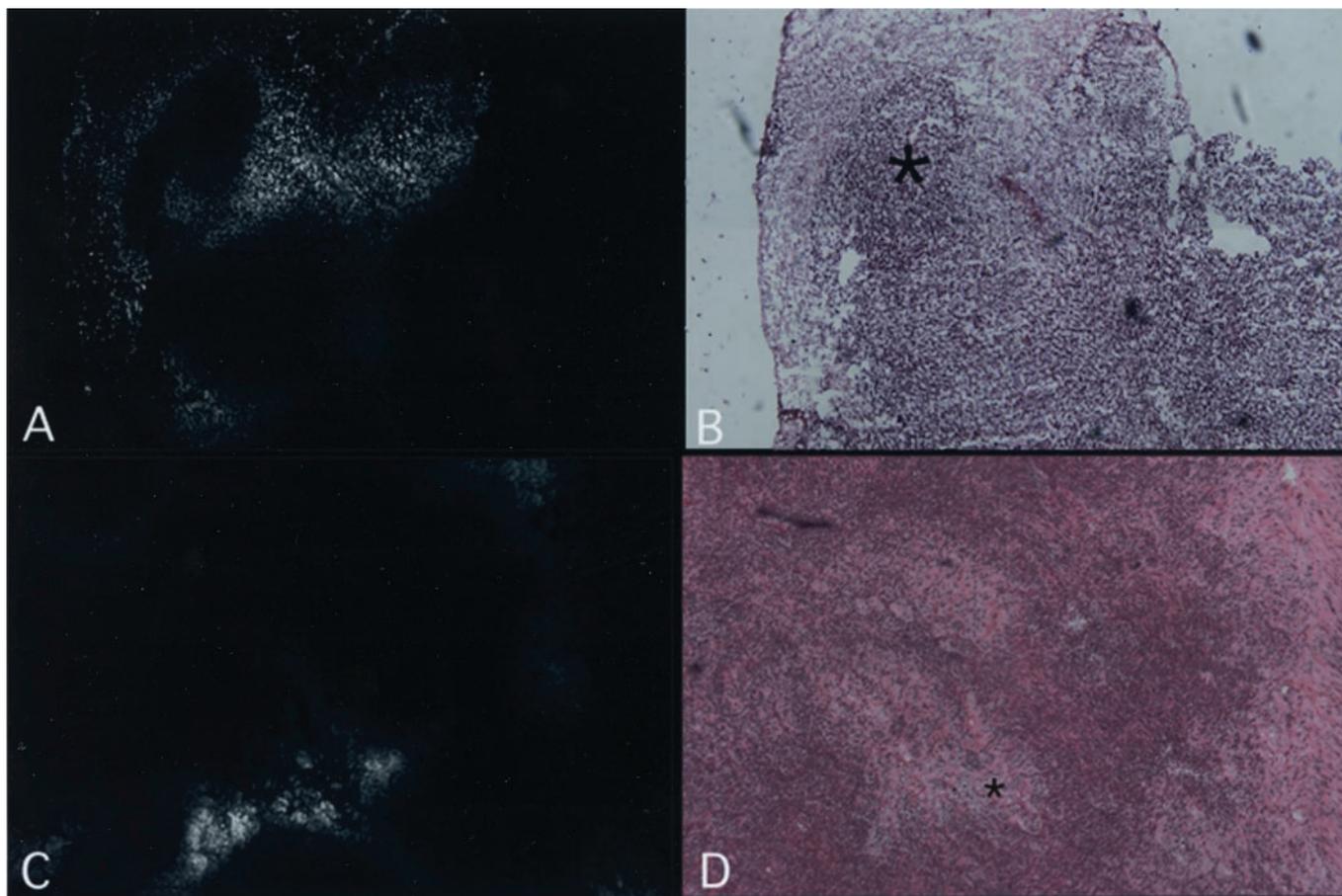
Fig. 2. Photomicrographs comparing patterns of EF5 binding and H&E counterstaining in two soft tissue sarcomas. Image intensity has been modified to demonstrate distribution of binding. However, absolute intensities are noted in Tables 1 and 2. (A, B) 2.0 × 1.4 mm; patient no. 16. Regions of very bright binding are seen adjacent to a macroscopic region of necrosis (large black *). (C, D) 2.0 × 1.4 mm; patient no. 10. A cluster of high-binding cells are seen in a region of microscopic necrosis (small black *). In adjacent regions, nonbinding, oxic cells are present.

usually not in the same studies. Because hypoxia itself has been shown to predict treatment failure (6), it is important to compare multiple markers (including hypoxia) with analysis of patient outcome. Improved access to hypoxia measurements for routine clinical usage is consequently desirable.

A number of techniques are available for measuring the presence of hypoxia in tumors *in vivo*. The needle electrode technique has been the most commonly used in clinical settings and reported studies have been pivotal in demonstrating an association between the presence of hypoxia and outcome

Table 2. Histological evaluation of tumors

Patient no.	Site	Histology	Grade	Size (cm)	% Necrosis	Mitoses/ 10 HPF	% of reference EF5 binding*
2	E	Desmoid	Low	6	0	2	14.0
10	E	Leiomyosarcoma	High	7	30	10	91.3
11	T	Leiomyosarcoma	High	11	50	42	27.8
8	T	MFH	High	11	10	20	99.3
16	RP	Synovial cell sarcoma	High	19	20	20	24.8
12	SB	GIST	High	0.5	3	14	5.1
				1.65			15.0
				> 6			10.7
9	SB	GIST	Low	0.8	0	4	8.2
20	SB	GIST	High	0.5	0	1	2.1

*Relative binding refers to percent of cube (reference) binding, corrected for AUC. In a patient where cube values were not available, an average EF5 value of appropriate other cubes was used.

Abbreviations: NE = not evaluated; GIST = gastrointestinal stroma tumor; MHF = malignant fibrous histiocytoma; RP = retroperitoneal; T = trunkal, E = extremity; SB = small bowel; HPF = high-power field.
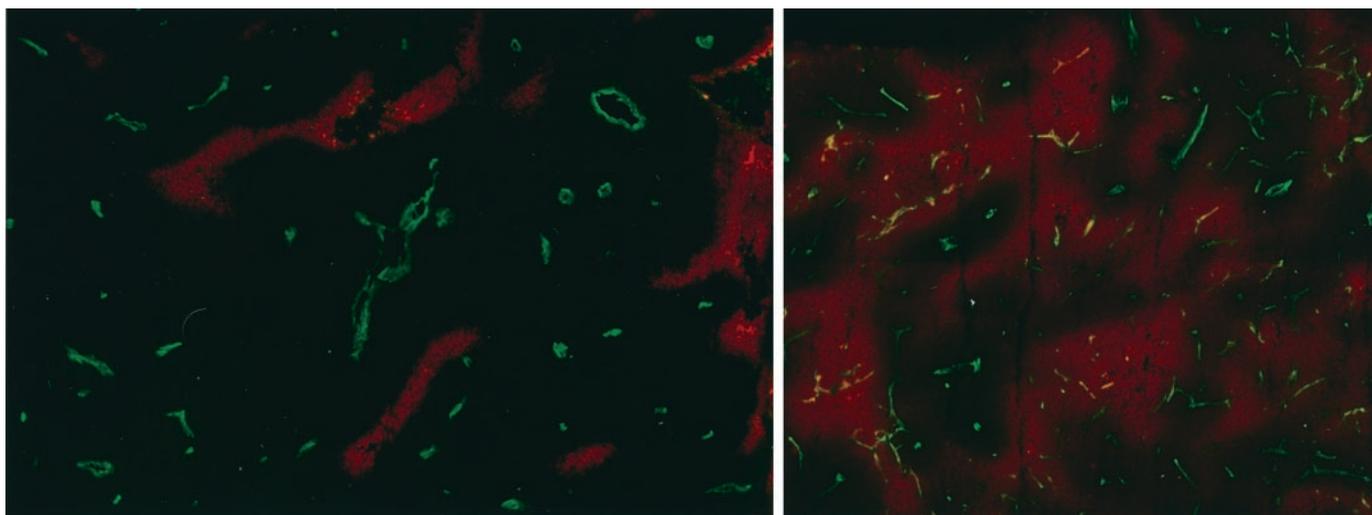
Fig. 3. Photomicrographs showing relative localization of blood vessels (stained with CD31/PECAM, green) and hypoxia (EF5, red) in two GISTs from patient no. 12. For fractional levels of binding, see Table 1. (A) 2.0 × 1.4 mm. This section was made from a 1.65-cm nodule on the small bowel. High EF5 binding is seen associated with regions of tumor necrosis. These binding regions are seen at a distance from blood vessels, compatible with diffusion limited hypoxia (B) 2.0 × 1.4 mm. This section was made from the central region of a large (6 cm) porta hepatis mass. In this area of the tumor, necrosis is not present. Low levels of EF5 binding can be seen directly adjacent to blood vessels. Areas of diffusion limited hypoxia are also seen.

(34, 36, 37). Despite its predictive success, the Eppendorf oxygen monitoring system is limited in it's application due to the inability to gain access for measurement in many tumor sites and the high degree of technical/medical expertise and associated costs required for successful measurements. Thus, new and simpler assays are required for further progress in our understanding of tumor hypoxia. 2-nitroimidazole-binding studies provide hypoxia measurements to virtually any degree of spatial resolution and with a multiplicity of detection techniques (18, 38–43). One strength of the nitroimidazole binding
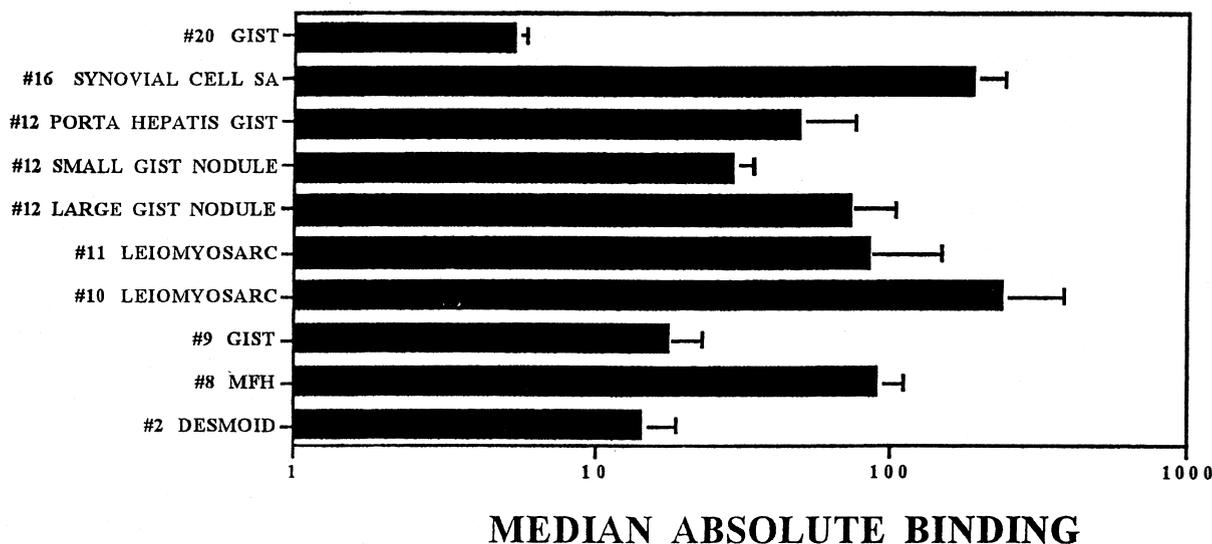

MEDIAN ABSOLUTE BINDING

Fig. 4. Intra and intertumoral heterogeneity of EF5 binding. The median value of the *absolute* binding levels in each of the tumors is shown. At least four sections from each tumor were evaluated for the brightest region of binding on the frozen sections, and the median ± SD was graphed. The variability between the individual sections is small, suggesting little intratumoral variability. In contrast, there is substantial variability in the binding levels between the various tumors, e.g., intertumoral heterogeneity. For patient no. 12, the binding values for each of the three separate tumor masses are listed separately.

Table 3. Eppendorf data

Patient no	Site	Histology	% Values less than 2.5 mm O_2	% Values less than 5-mm O_3	% Values less than 10-mm O_2
2	E	Desmoid	27	79	79
10	E	Leiomyosarcoma	85	85	86
11	T	Leiomyosarcoma	59	65	70
8	T	MFH	26	29	68
16	RP	Synovial cell sarcoma	26	29	68
12	SB	GIST	ND	ND	ND
9	SB	GIST	ND	ND	ND
20	SB	GIST	ND	ND	ND

Abbreviations: ND = not done; GIST = gastrointestinal stroma tumor; MFH = malignant fibrous histiocytoma; RP = retroperitoneal; T = trunkal; E = extremity; SB = small bowel.

technique is that a signal for dead cells is not generated because these cells do not metabolize the drug. The binding techniques also have maximum sensitivity at low pO_2, thus providing a positive signal in the absence of oxygen. Our methods using the 2-nitroimidazole drug EF5 allow estimation of not only the *presence* of hypoxia, but the *level* of hypoxia by comparing *in situ* binding to a reference binding level (16). We have previously demonstrated that in squamous cell tumors, such as the STS tumors reported herein, intratumoral heterogeneity was large, extending from minimal fluorescence up to 88.6% of reference binding. In tumors with minimal binding, there was

little intratumoral heterogeneity. Taken together, these studies demonstrated substantial heterogeneity of brightest *in situ* binding between and within individuals tumors of very different histologies and sites. The clinical relevance of evaluating the region of brightest binding must be further studied. However, the rationale for choosing this endpoint was our hypothesis that the response to therapy would be determined by the most resistant, e.g., hypoxic cells.

All of the patients with GIST tumors had recurrent disease at the time of their EF5 study. In the 2 patients that received a laparoscopy, the extent of the disease could not

EF5 BINDING vs. EPPENDORF ELECTRODE VALUES IN SOFT TISSUE SARCOMAS
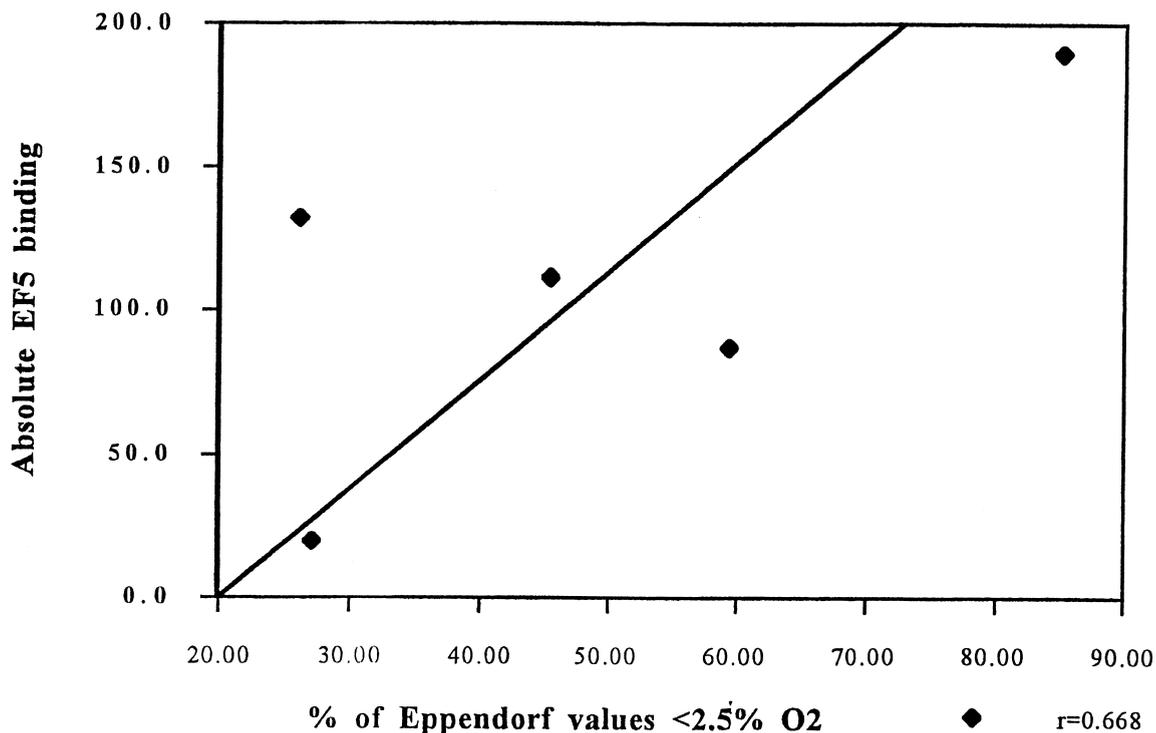

Fig. 5. Comparison of percent reference EF5 binding and Eppendorf measurements expressed as percentage of values less than 2.5 mmHg. A trend toward higher EF5 binding and percent values less than 2.5 mmHg is seen. $r = 0.67$.

be determined and only very small nodules were sampled; these had low binding. In the third GIST patient (#12), a laparotomy was performed and nodules were taken from various sized (<1 cm - 6 cm) masses. Heterogeneity of binding within and between these masses was seen (Fig. 5). In a 1.65 cm nodule, necrosis was present and diffusion-limited, severe hypoxia was demonstrated by high levels of EF5 binding (Fig. 3a). In a non-necrotic region of the larger mass, lower levels EF5 binding was present suggesting low-intermediate levels of hypoxia adjacent to vessels (Table 1, Fig. 3b). The interpretation of this observation is complex because the binding that is seen is an integration of the time and tissue-drug exposure level over the 48 h between drug administration and surgical extirpation. As well, these studies do not allow assessment of the blood vessel functionality, i.e., vasomotion, nor evaluation of the oxygen saturation within the blood (22). Such studies are only possible in rodent systems at this time (44, 45). Nonetheless, additional studies of multiple nodules of varying size and conformation should be done to further characterize this type of heterogeneity in human tumors.

Because the reported study is a Phase I trial, the number of patients is not extensive. Nonetheless, in 5 patients with non-GIST sarcomas, a correspondence of EF5 binding with percentage of Eppendorf electrode values less than 2.5-mmHg values was identified. In previous Eppendorf studies, the median pO$_2$ value, and therefore the "cutoff" used, ranged from 2.5 mmHg in head and neck squamous cell tumors to 10 mmHg in STS (6, 37). Values of ≤ 2.5 mmHg correspond with intermediate to severe hypoxia. Some authors have suggested that intermediately hypoxic tumor cells are most important in determining outcome for radiation response (10, 46, 47). Presumably, this would be most relevant to outcome in cancer patients treated with radiation therapy, as in the head and neck patients studied by Nordsmark (48). It is not well understood what oxygen levels or circumstances would be necessary to cause molecular/biologic changes that would predispose a STS to metastasize.

The techniques described herein allow quantitation of the *pattern and area as well as the level of binding*. Further studies will be necessary to determine which of these, or a combination thereof, will provide the optimal description of hypoxia. The eventual goal of these studies will be to determine whether such EF5 binding studies can predict patient outcome. This is particularly relevant to STS patients because the major cause of mortality is distant metastasis, for which there is currently no efficacious therapy. If the population of patients at highest risk for metastasis can be identified using EF5 binding studies, better studies can be designed to identify optimal systemic therapies.

REFERENCES

1. Stone HB, Brown JM, Phillips TL, *et al*. Oxygen in human tumors: Correlations between methods of measurement and response to therapy. Summary of a workshop held November 19–20, 1992, National Cancer Institute, Bethesda, Maryland. *Radiat Res* 1993;136:422–434.
2. Overgaard J. Clinical evaluation of nitroimidazoles as modifiers of hypoxia in solid tumors. *Oncol Res* 1994;6:509–518.
3. Brown JM. SR 4233 (tirapazamine): A new anticancer drug exploiting hypoxia in solid tumours. *Br J Cancer* 1993;67:1163–1170.
4. Rojas A. ARCON: Accelerated radiotherapy with carbogen and nicotinamide. *Br J Radiol 1992;24(Suppl.):174–178.*
5. Hockel M, Knoop C, Schlenger K, *et al*. Intratumoral pO2 predicts survival in advanced cancer of the uterine cervix. *Radiother Oncol* 1993;26:45–50.
6. Brizel DM, Scully SP, Harrelson JM, *et al*. Tumor oxygenation predicts for the likelihood of distant metastases in human soft tissue sarcoma. *Cancer Res* 1996;56:941–943.
7. Reynolds TY, Rockwell S, Glazer PM. Genetic instability induced by the tumor microenvironment. *Cancer Res* 1996;56:5754–5757.
8. Graeber TG, Osmanian C, Jacks T, *et al*. Hypoxia-mediated selection of cells with diminished apoptotic potential in solid tumours [see comments]. *Nature* 1996;379:88–91.
9. Young SD, Marshall RS, Hill RP. Hypoxia induces DNA overreplication and enhances metastatic potential of murine tumor cells. *Proc Natl Acad Sci USA* 1988;85:9533–9537.
10. Evans SM, Jenkins WT, Joiner B, *et al*. 2-Nitroimidazole (EF5) binding predicts radiation resistance in individual 9L s.c. tumors, *Cancer Res* 1996;56:405–411.
11. Evans SM, Laughlin KM, Pugh CR, *et al*. Use of power Doppler ultrasound-guided biopsies to locate regions of tumour hypoxia. *Br J Cancer* 1997;76:1308–1314.
12. Evans SM, Koch CJ, Laughlin KM, *et al*. Tamoxifen induces hypoxia in MCF-7 xenografts. *Cancer Res* 1997;57:5155–5161.
13. Lee J, Siemann DW, Koch CJ, *et al*. Direct relationship between radiobiological hypoxia in tumors and monoclonal antibody detection of EF5 cellular adducts. *Int J Cancer* 1996;67:372–378.
14. Siim BG, Menke DR, Dorie MJ, *et al*. Tirapazamine-induced cytotoxicity and DNA damage in transplanted tumors: Relationship to tumor hypoxia. *Cancer Res* 1997;57:2922–2928.
15. Kavanagh MC, Tsang V, Chow S, *et al*. A comparison in individual murine tumors of techniques for measuring oxygen levels. *Int J Radiat Oncol Biol Phys* 1999;44:1137–1146.
16. Evans S, Hahn S, Pook D, *et al*. Detection of hypoxia in human squamous cell carcinoma by EF5 binding. *Cancer Res* 2000;60:2018–2024.
17. Koch C, Hahn S, Rockwell K, *et al*. Pharmacokinetics of the 2-nitroimidazole EF5 ([2-(2-nitro-1-H-imidazole-1-yl)-N-(2,2,3,3,3-pentafluoropropyl)acetamide] in human patients: Implications for hypoxia measurements *in vivo*. *Clin Cancer Res*. Submitted.
18. Evans SM, Joiner B, Jenkins WT, *et al*. Identification of hypoxia in cells and tissues of epigastric 9L rat glioma using EF5 [2-(2-nitro-1H-imidazol-1-yl)-N-(2,2,3,3,3-pentafluoropropyl) acetamide]. *Br J Cancer* 1995;72:875–882.
19. Koch CJ, Evans SM, Lord EM. Oxygen dependence of cellular uptake of EF5 [2-(2-nitro-1H-imidazol-1-yl)-N-(2,2,3,3,3-pentafluoropropyl)acetamide]: Analysis of drug adducts by fluorescent antibodies vs. bound radioactivity. *Br J Cancer* 1995;72:869–874.
20. Saunders MJ, Dische S, Anderson P, *et al*. The neurotoxicity of misonidazole and its relationship to dose, half-life and concentration in the serum. *Br J Cancer* 1979;37:268–270.

21. Laughlin KM, Evans SM, Jenkins WT, *et al*. Biodistribution of the nitroimidazole EF5 (2-[2-nitro-1H-imidazol-1-yl]-N-(2,2,3,3,3-pentafluoropropyl) acetamide) in mice bearing subcutaneous EMT6 tumors. *J Pharmacol Exp Ther* 1996;277: 1049–1057.

22. Dewhirst MW, Kimura H, Rehmus SW, *et al*. Microvascular studies on the origins of perfusion-limited hypoxia. *Br J Cancer* 1996.27(Suppl.):S247–251.

23. Landis SH, Murray T, Bolden S, *et al*. Cancer statistics, 1999. [see comments]. *CA Cancer J Clin* 1999;49:8–31.

24. Dirix L, Van Oosterom, A. Soft tissue sarcomas in adults. *Curr Opin Oncol* 1999;11:285–295.

25. LeVay J, O'Sullivan B, Catton C, *et al*. Outcome and prognostic factors in soft tissue sarcoma in the adult. *Int J Radiat Oncol Biol Phys* 1993;27:1091–1099.

26. Costa J, Wesley RA, Glatstein E, *et al*. The grading of soft tissue sarcomas. Results of a clinicohistopathologic correlation in a series of 163 cases. *Cancer* 1984;53:530–541.

27. Pisters PW, Leung DH, Woodruff J, *et al*. Analysis of prognostic factors in 1,041 patients with localized soft tissue sarcomas of the extremities. *J Clin Oncol* 1996;14:1679–1689.

28. Drobnjak M, Latres E, Pollack D, *et al*. Prognostic implications of p53 nuclear overexpression and high proliferation index of Ki-67 in adult soft-tissue sarcomas. *J Natl Cancer Inst* 1994;86:549–554.

29. Hlatky L, Tsionou C, Hahnfeldt P, *et al*. Mammary fibroblasts may influence breast tumor angiogenesis via hypoxia-induced vascular endothelial growth factor up-regulation and protein expression. *Cancer Res* 1994;54:6083–6086.

30. Lyng H, Sundfor K, Rofstad EK. Oxygen tension in human tumours measured with polarographic needle electrodes and its relationship to vascular density, necrosis and hypoxia. *Radiother Oncol* 1997;44:163–169.

31. Cooper RA, Wilks DP, Logue JP, *et al*. High tumor angiogenesis is associated with poorer survival in carcinoma of the cervix treated with radiotherapy. *Clin Cancer Res* 1998;4: 2795–2800.

32. Goulding H, Jasani B, Pereira H, *et al*. Metallothionein expression in human breast cancer. *Br J Cancer* 1995;72:968–972.

33. Raleigh JA, Chou SC, Tables L, *et al*. Relationship of hypoxia to metallothionein expression in murine tumors. *Int J Radiat Oncol Biol Phys* 1998;42:727–730.

34. Nordsmark M, Hoyer M, Keller J, *et al*. The relationship between tumor oxygenation and cell proliferation in human soft tissue sarcomas. *Int J Radiat Oncol Biol Phys* 1996;35: 701–708.

35. Raybaud-Diogene H, Fortin A, Morency R, *et al*. Markers of radioresistance in squamous cell carcinomas of the head and neck: A clinicopathologic and immunohistochemical study. *J Clin Oncol* 1997;15:1030–1038.

36. Hockel M, Schlenger K, Aral B, *et al*. Association between tumor hypoxia and malignant progression in advanced cancer of the uterine cervix. *Cancer Res* 1996;56:4509–4515.

37. Brizel DM, Sibley GS, Prosnitz LR, *et al*. Tumor hypoxia adversely affects the prognosis of carcinoma of the head and neck. *Int J Radiat Oncol Biol Phys* 1997;38:285–289.

38. Cline JM, Thrall DE, Page RL, *et al*. Immunohistochemical detection of a hypoxia marker in spontaneous canine tumours. *Br J Cancer* 1990;62:925–931.

39. Evans SM, Kachur AV, Shiue CY, *et al*. Noninvasive detection of tumor hypoxia using the 2-nitroimidazole [18F]EF1. *J Nucl Med* 2000;41:327–336.

40. Franko AJ, Koch CJ, Garrecht BM, *et al*. Oxygen dependence of binding of misonidazole to rodent and human tumors in vitro. *Cancer Res* 1987;47:5367–5376.

41. Hodgkiss RJ, Middleton RW, Parrick J, *et al*. Bioreductive fluorescent markers for hypoxic cells: A study of 2-nitroimidazoles with 1-substituents containing fluorescent, bridgehead-nitrogen, bicyclic systems. *J Med Chem* 1992;35:1920–1926.

42. Koh WJ, Bergman KS, Rasey JS, *et al*. Evaluation of oxygenation status during fractionated radiotherapy in human nonsmall cell lung cancers using [F-18]fluoromisonidazole positron emission tomography. *Int J Radiat Oncol Biol Phys* 1995;33:391–398.

43. Olive PL, Durand RE. Fluorescent nitroheterocycles for identifying hypoxic cells. *Cancer Res* 1983;43:3276–3280.

44. Fenton BM, Paoni SF, Lee J, *et al*. Quantification of tumour vasculature and hypoxia by immunohistochemical staining and HbO2 saturation measurements. *Br J Cancer* 1999;79: 464–471.

45. Wilson DF, Cerniglia GJ. Localization of tumors and evaluation of their state of oxygenation by phosphorescense imaging. *Cancer Res* 1992;52:3988–3993.

46. Wouters BG, Brown JM. Cells at intermediate oxygen levels can be more important than the "hypoxic fraction" in determining tumor response to fractionated radiation therapy. *Radiat Res* 1997;147:541–550.

47. Evans SM, Jenkins WT, Shapiro M, *et al*. Evaluation of the concept of "hypoxic fraction" as a descriptor of tumor oxygenation status. *Adv Exp Med Biol* 1997;411:215–225.

48. Nordsmark M, Overgaard M, Overgaard, J. Pretreatment oxygenation predicts radiation response in advanced squamous cell carcinoma of the head and neck. *Radiother Oncol* 1996; 41:31–39.